Polo-Like Kinase 1 Depletion Induces DNA Damage in Early S Prior to Caspase Activation

Citation

Published Version

Permanent link

Terms of Use

Share Your Story

Polo-like kinase-1 depletion induces DNA damage in early S

prior to caspase activation

Hyungshin Yim[*] and Raymond L. Erikson

Department of Molecular and Cellular Biology, Harvard University, Cambridge, Massachusetts 02138, USA

[*]Corresponding author

Phone: +1-617-495-5386

Fax: +1-617-495-0681

E-mail: hyim@fas.harvard.edu

Running title: DNA damage by Plk1 depletion in early S

Keywords: Plk1, S phase, DNA damage, apoptosis.

Introduction, Results, and Discussion sections: 4,353 words

Materials and methods section: 1,188 words

ABSTRACT

Polo-like kinase 1 (Plk1) plays several roles in mitosis, and it has been suggested to have a role in tumorigenesis. We have previously reported that Plk1 depletion results in cell death in cancer cells, whereas normal cells survive similar depletion. However, Plk1 depletion together with p53 depletion induces cell death in normal cells as well. This communication presents evidence on the sequence of events that leads to cell death in cancer cells. DNA damage is detected at the first S phase following Plk1 depletion and is more severe in Plk1-depleted p53-null cancer cells. As a consequence of Plk1 depletion using lentivirus-based siRNA techniques, pre-replicative complex (pre-RC) formation is disrupted at the G1/S transition and DNA synthesis is reduced during S phase of the first cycle after depletion. The levels of geminin, an inhibitor of DNA pre-RC, and Emi1, an inhibitor of APC/C, are elevated in Plk1-depleted cells. The rate of cell cycling is slower in Plk1-depleted cells than in control cells when synchronized by serum starvation. Plk1 depletion results in disrupted DNA pre-RC, reduced DNA synthesis and DNA damage before cells display severe mitotic catastrophe or apoptosis. Our data suggest that Plk1 is required for cell cycle progression not only in mitosis but also for DNA synthesis, maintenance of DNA integrity and prevention of cell death.

INTRODUCTION

Progression of the cell cycle is tightly regulated in eukaryotic cells by coordinated control of phosphorylation and proteolytic events. Duplication of genetic information for the next cell generation requires the precise coordination of numerous proteins (2). To ensure the accurate division of duplicated DNA, cells require condensed chromosomes, a mitotic spindle, and correct attachment of duplicated chromosomes to the spindle. Errors in DNA replication and mitosis may lead to cell death through apoptosis or result in mutations that lead to cancer (3). Polo-like kinase 1 (Plk1) is essential for several steps in mitosis, and is highly expressed in proliferating cells. Expression of Plk1 increases in S phase and peaks during M phase (8). In addition, at the G2/M boundary Plk1 is activated by phosphorylation and promotes mitotic entry. Its primary role in mammalian cells appears to be control of mitotic progression, particularly in the metaphase-anaphase transition, and mitotic exit (37). At the G2/M transition, Plx1, a counterpart of Plk1 in *Xenopus*, activates cyclin B1/Cdk1 by phosphorylation of Cdc25C (14), or of cyclin B1 (29). During mitotic entry, Plk1 is required for recruitment of the γ-tubulin ring complex (7). Phosphorylation of Emi1 by Plk1 leads to its destruction, release of Cdc20, and activation of the anaphase-promoting complex/cyclosome (APC/C) (10, 22, 26). Active APC/C mediates the degradation of proteins such as cyclin A, cyclin B1, securin, and geminin to promote exit from mitosis (6, 26). The multiple roles of Plk1 from the entry to and exit from mitosis indicate its importance as a regulator of these events.

Recently several reports suggest that Plk1 may play a role in other phases of the cell cycle. Plk1 interacts with pre-replicative complex proteins, such as Mcm2 and Orc2, in

yeast two-hybrid studies (32), and coimmunoprecipitates with Mcm2-7 and Orc2 (32, 35). Orc2, Mcm4, Mcm6 and Mcm7 proteins colocalize in the centrosome with Plk1 (25, 32). In addition, ectopic expression of Plk1-S137D arrests HeLa cells at the G1/S boundary (12). Moreover, microinjection of *in vitro* transcribed sense mRNA of Plk1 into serum-starved NIH 3T3 cells induced thymidine incorporation, whereas microinjection of antisense mRNA into growing NIH 3T3 cells that were stimulated with serum blocked thymidine incorporation (9). This observation suggests that Plk1 is required for DNA synthesis and that overexpression of Plk1 appears to be sufficient for induction of DNA synthesis. These data raise the possibility that Plk1 might have a required function in DNA replication.

Depletion of Plk1 activity by microinjection of neutralizing anti-Plk1 antibody impairs centrosome maturation in HeLa cells (15). When Plk1 function is blocked by dominant-negative Plk1, several human tumor cells undergo mitotic catastrophe independent of Cdc25C (1). In Plk1-deficient human cancer cells, centrosomes do not separate to form bipolar spindles. The cells undergo prometaphase arrest and cell death caused by mitotic catastrophe (18, 33, 38). These effects are more severe in p53-deficient cancer cells. Cells co-depleted for p53 and Plk1 undergo cell death as a consequence of mitotic defects (17). However, it is unclear how Plk1 depletion induces cell death or what the sequence of events is prior to cell death.

Here, we provide evidence that Plk1 depletion induces DNA damage at G1/S before cell death responses such as caspase activation are initiated.

4

RESULTS

The formation of γ-H2A.X foci precedes the activation of caspase-3 in Plk1-depleted cancer cells.

In previous studies, we reported that the Plk1-depleted cancer cells undergo apoptosis (17, 18). FACS analysis and activation of caspase-3 showed that Plk1 depletion induced severe apoptosis in puromycin-selected cells 3-5 days after infection of Plk1 targeting lentivirus (P) compared with control virus carrying the pLKO-puro.1 vector (C) in HeLa cells (Supplementary Fig. 1, A-B). Lentivirus-expressing mutant RNAi sequence target of Plk1 (M) was used for the off-target control. Histone H2A.X was phosphorylated and cleaved caspase-3 was detected at 3 days after Plk1 depletion whereas the ratio of γ-H2A.X-positive cells or cleaved caspase-3-positive cells was low in vector control or off-target control (Supplementary Fig. 1, C- D), which suggests that DNA damage and apoptosis occurred in Plk1-depleted cancer cells. However, the sequence of events was unclear.

To investigate this issue, lentivirus-infected cells were not selected by puromycin because the infection efficiency was very high and the treatment of puromycin could influence the DNA damage response and also cells were observed within 48 h after infection (Supplementary Fig. 2A). Because caspase-3 was activated at 24-48 h after release as measured by enzyme assay using caspase-3 specific substrate in Plk1-depleted puromycin non-selected HeLa cells (Supplementary Fig. 2, A-B), virus-infected cells were observed from 0 h to 24 h after release (from 24 h to 48 h after infection). In order to determine the sequence of events following Plk1 depletion, the formation of γ-H2A.X foci and the activation of caspase-3 were measured (Fig. 1). The

level of Plk1 depletion was checked by immunoblot (Fig. 1A), and the cell cycle was followed with FACS analysis (Fig. 1B). As expected, cycling was slower in Plk1-depleted cells than in control cells, and the population of subgenomic DNA, an indication of apoptosis, increased beginning at 24 h in Plk1-depleted cells (Fig. 1B). Caspase-3 activity was elevated 2-fold in Plk1-depleted cells relative to control cells at 24 h (Supplementary Fig. 2B). In addition, γ-H2A.X foci-positive cells were visible at 0 h (24 h after infection) in Plk1-depleted cells and the population of γ-H2A.X foci-positive cells increased with time as compared with control virus-infected cells (Fig. 1, C and D). In contrast, cleaved caspase-3 was not detected until 12 h (Fig. 1, C and E). To support the association of Plk1 depletion and H2A.X phosphorylation, Plk1-depleted mitotic cells were stained with anti-p-histone H2A.X (Ser139) antibody at 10 h after release from the double thymidine block. As shown in Supplementary Fig. 3, H2A.X protein was phosphorylated in Plk1-depleted cells.

The involvement of p53 in DNA damage and apoptosis by Plk1 depletion and the dependency on p73 in p53-deficient cells.

To analyze the involvement of p53 in DNA damage and cell death following Plk1 depletion, these experiments were repeated with U2OS cells (p53 wild type), Saos2 (p53 null), and H1299 (p53 null) cells. As was the case with HeLa, γ-H2A.X foci-positive cells were already visible at the end of the double thymidine block in Plk1-depleted cells and the percentage of γ-H2A.X foci-positive cells increased with time compared with control virus-infected cells (Fig. 2A). Activated caspase-3 was detected between 12 h to 24 h after release, later than the formation of γ-H2A.X foci and this pattern was p53-independent (Fig. 2, A and B). In H1299 cells, apoptosis was severe, as

6

shown subgenomic DNA content (Fig. 2C).

In order to obtain evidence of checkpoint activation in p53-null cells, we analyzed the level of phosphorylated Chk2 on T68 in Plk1-depleted H1299 p53-null cells. As shown in Figure 2D, Chk2 was phosphorylated by the end of the second thymidine block and the level of p-Chk2 increased with time. These data are consistent with the timing of γ-H2A.X foci formation (Fig. 1C, 1E and 2A). In contrast, Chk1 phosphorylation was not detected until 24 h after release from the double thymidine block in Plk1-depleted cells (Fig. 2D). Chk2 drives E2F1 activation and p73 expression, which in turn induce expression of pro-apoptotic proteins such as Bax and Apaf-1 in p53-independent apoptotic progression (27). The protein levels of E2F-1 and p73 were analyzed by western blot (Fig. 2D). As expected, p53 protein was not detected (unpublished data). The protein levels of E2F-1, a target of Chk2, and of p73 were elevated by the end of second thymidine block in Plk1-depleted H1299 cells.

We examined the influence of p73 on apoptosis in Plk1-depleted H1299 cells (Fig. 2, E-G). Twenty hours after release from the double thymidine block, depletion of p73 reduced the level of subgenomic DNA induced by Plk1 depletion in H1299 cells as determined by FACS analysis (Fig. 2, E-F). In addition, twelve hours after release from the double thymidine block, the transfection of p73 siRNA reduced the expression of Bax in control cells, while the level of Bax showed only a modest increase in Plk1-depleted cells (Fig. 2G). These data suggest that Plk1 depletion resulted in DNA damage at the G1/S transition, and activated the Chk2-E2F1-p73 checkpoint-signaling pathway. This activation may contribute to apoptosis through the expression of Bax mediated by p73 in p53-null cells.

DNA damage is induced in early S phase in Plk1-depleted cancer cells.

As shown in Figure 2D, checkpoint signaling was activated at the G1/S transition in Plk1-depleted p53-null cells. To further confirm that DNA damage occurs in early S phase, a comet assay was carried out in Plk1-depleted HeLa cells that were synchronized by the double thymidine block and treated with hydroxyurea to arrest them in G1/early S phase. At 0 h after release from the second thymidine block, 14% of Plk1-depleted cells displayed a comet-like shape, which is an independent measure of DNA damage (21) (Fig. 3, A and B). This percentage increased up to 27% at 6 h when the cells were in G2/M phase. When cells were treated with hydroxyurea after the double thymidine block, the population of comet-tailing cells was 13% in Plk1-depleted cells (*versus* 5% in control cells) (Fig. 3B). FACS analysis was performed to confirm the cell cycle phase (Fig. 3C).

We also assessed the percentage of γ-H2A.X foci-positive cells over time after release from the double thymidine block (Fig. 3D). Consistently, upon Plk1 depletion the percentage of γ-H2A.X foci-positive cells was elevated at 0-2 h in early S phase as judging FACS analysis, and at 6 h after release increased 3-fold compared to control cells. These results show that Plk1 depletion does induce DNA damage in early S phase, however the effect in G2/M is greater.

Plk1 depletion disrupts the binding of Mcm proteins to chromatin.

The above data indicate that Plk1 depletion induced DNA damage not only in G2/M but also in S phase. It is well known that Plk1 plays multiple and critical roles in mitosis but only recently have some reports suggested that Plk1 may have a function in S phase (32, 35). We found DNA synthesis in Plk1-depleted HeLa cells was about one-half that in

control cells at 2 h after release as determined by BrdU incorporation for 30 min (Fig. 4, A and B). However, incorporation of BrdU for 60 min was not markedly reduced in Plk1-depleted cells compared to that of control cells. These data indicate that DNA synthesis was not completed blocked but slowly occurred at the early time after Plk1 depletion.

To address how Plk1 depletion may influence DNA synthesis, chromatin-binding assays were performed to observe pre-RC formation. At 2 h after release from the double thymidine block, cells were collected and fractionated into soluble and chromatin fractions. As shown in Figure 4C, the level of chromatin-bound Mcm7 was decreased and conversely, the level of soluble Mcm7 was increased in Plk1-depleted cells as compared with in control. As was the case with Mcm7, the level of chromatin-bound Mcm3 was also decreased in Plk1-depleted cells compared with control (Fig. 4C). To determine whether Plk1 kinase influences loading Mcm proteins on pre-RC, a chromatin binding assay was performed. pEGFP-mouse-Plk1 wild type (WT) or kinase defective Plk1 (K82M) was transfected in Plk1-depleted or control HeLa cells. Two hours after release from the double thymidine block, the level of chromatin-bound Mcm7 decreased when Plk1-KM was expressed in control and Plk1-depleted cells (Fig. 4D). In Plk1-depleted cells, the level of chromatin-bound Mcm7 increased when Plk1-WT was expressed compared to GFP-mock transfected cells. The reduction of chromatin-bound Mcm7 caused by Plk1 depletion was restored by expression of Plk1-WT. These data indicate that Plk1 plays a role in the loading of Mcm proteins on Pre-RC.

The activity of ATM, a DNA damage-sensing kinase, was significantly activated within 2 h after release from the double thymidine block in Plk1-depleted cells (Fig. 4E, left

9

panel). ATR which is activated as a result of stalled DNA replication was modestly activated at this point (Fig. 4E, right panel). These data indicate that Plk1 depletion disrupted Mcm proteins binding to chromatin in early S phase, presumably affecting DNA synthesis. Thus, Plk1 depletion may result in DNA damage caused by disruption of the pre-replication complex.

Disruption of the pre-RC by Plk1 depletion is associated with the accumulation of Emi1 and geminin.

To investigate the mechanism that leads to disruption of pre-RC, the protein level of geminin, an inhibitor of Cdt1 in pre-RC and a target of anaphase promoting complex/cyclosome (APC/C), was determined by western blot. During mitosis, Plk1 phosphorylates Emi1, an inhibitor of APC/C. Thus Emi1 protein is degraded mediated by phosphorylation and APC/C is no longer inhibited (10, 22). Plk1 depletion may stabilize Emi1 and consequently, the degradation of geminin would be reduced. As expected, the levels of geminin and Emi1 were greater in Plk1-depleted cells than in control cells at the end of the second thymidine block (Fig. 5A). At the same time, the kinase ATM, a DNA damage-sensing kinase, was phosphorylated on S1981 in Plk1-depleted cells. In addition, Chk2, a DNA damage signaling kinase, was phosphorylated on T68 in Plk1-depleted cells although the protein level of Chk2 was not altered (Fig. 5A). We determined whether Emi1 protein level is directly affected by the protein level and kinase activity of Plk1. pEGFP-mouse-Plk1-WT or kinase defective mutant was transfected into the Plk1-depleted or control HeLa cells, and the protein level of Emi1 was observed by immunohistochemistry at 2 h after release from the double thymidine block (Fig. 5B). The intensity of the immunofluorescent signal of Emi1 increased in

10

Plk1-depleted cells compared with that of control cells (Fig. 5B). In GFP expressed cells, the level of Emi1 was not altered between transfected and nontransfected cells in both control- or Plk1-depleted cells. However, in GFP-tagged Plk1-WT expressed cells the level of Emi1 decreased compared with that of the non-transfected cells. While, the level of Emi1 significantly increased in GFP-Plk1-kinase defective mutant (KM)-expressed cells compared with that of non-transfected cells cells in both control- or Plk1-depleted cells.

In Plk1-depleted cells, the increased level of Emi1 by Plk1 depletion was recovered by expression of GFP-Plk1-WT. However, the expression of Plk1 kinase defective mutant significantly increased the level of Emi1 (Fig. 5B). In addition, the levels of Emi1 and geminin were checked by western blot (Supplementary Fig.4S). In control virus-infected cells, the level of Emi1 decreased when Plk1-wt was expressed (Supplementary Fig. 4S), whereas levels of Emi1 and geminin increased in GFP-Plk1-KM expressing cells. In Plk1-depleted cells, the levels of Emi1 and geminin slightly decreased when pEGFP-Plk1-wt was expressed whereas, the levels increased in cells expressing Plk1-KM (Supplementary Fig. 4S). These results suggest that Plk1 depletion causes the increase in the level of Emi1 and geminin as a consequence of the attenuation of their degradation, and that the increased level of geminin could inhibit pre-RC formation in Plk1-depleted cells.

To observe the correlation between the level of geminin and pre-RC disruption, chromatin binding assay and immunoprecipiation were performed. At 2h after release from the double thymidine block, the level of chromatin-bound Cdt1 was decreased in Plk1-depleted cells compared to control (Fig. 5C). The levels of soluble Cdt1 and geminin were increased and soluble Cdt1 was phosphorylated in Plk1-depleted cells.

Using this soluble fraction, geminin was immunoprecipitated and an immunoblot was performed with anti-Cdt1 antibody (Fig. 5D). As expected, soluble geminin bound to Cdt1 in Plk1-depleted cells. These data implied that stabilized soluble geminin binds Cdt1, reduced the chromation binding of Cdt1 to the pre-RC, and consequently disrupted pre-RC formation upon Plk1 depletion.

DNA damage occurred in G1/S and DNA synthesis was reduced in Plk1-depleted T98G cells.

T98G cells can efficiently be synchronized in G1 phase by serum starvation, which provides an alternative to the double thymidine approach to evaluate the influence of Plk1 depletion in G1/S phase. At 2 days after serum deprivation, the cells were infected with Plk1-targeting lentivirus for 1 day. Then the cells were stimulated by the addition of serum. The DNA damage response was checked by ATM activity. Consistent with the previous data, ATM kinase was activated at 12 h after serum release during early S phase in Plk1-depleted T98G cells (Fig. 6, A and C). The percentage of γ-H2A.X foci-positive cells was 7.8% at 12 h and then gradually increased up to 10% at 20 h after serum addition in Plk1-depleted T98G cells (Fig. 6, B and C). Moreover, the level of ATM phosphorylated on S1981 was much greater in Plk1-depleted cells than that of control cells at 16 h after serum stimulation as determined by western blot (Fig. 6F). Thus, ATM, which senses DNA damage was activated in G1/S when Plk1 was depleted in T98G cells. In addition, the G1/S peak was sharper in Plk1-depleted cells than in control cells at 12 h to 16 h (Fig. 6C). This result indicates that the cell cycling is much slower in Plk1-depleted cells than in control cells in early S phase. These results suggest that Plk1 depletion initially induced DNA damage in early S phase and this increased in

G2/M phase. The rate of DNA synthesis decreased to about 2% in Plk1-depleted T98G cells as compared with 70% in control cells at 16 h after release from serum starvation (Fig. 6, D and E). This inhibition was much more severe than that in HeLa cells synchronized by the double thymidine block (Fig. 6, D and E; Fig. 4, A and B).

We determined the levels of Emi1 and geminin in serum-starved T98G cells, and found the levels of Emi1 and geminin are greater in Plk1-depleted cells than those in control cells at 16 h after release from serum starvation (Fig. 6F). Thus, the level of Emi1 and geminin increased after Plk1 depletion in the serum starved T98G cells. In order to extend the observation that Emi1 accumulated in the Plk1-depleted HeLa cells, the Plk1-depleted T98G cells were synchronized with double thymidine block. The DNA-damage response was checked by phosphorylation of Chk2 kinase on T68. In consistent with the previous data, Chk2 was phosphorylated at 2 h after serum release during early S phase in Plk1-depleted T98G cells (Fig. 6G). At the same time, the level of Emi1 was greater in Plk1-depleted T98G cells than in control cells (Fig. 6G). Thus, Plk1 depletion did lead to increased levels of Emi1 and phosphorylated Chk2 in early S phase. These results show that Plk1 depletion caused the accumulation of Emi1 and induced the activation of Chk2 in T98G cells independent with synchronization method.

DISCUSSION

In this manuscript we describe studies on the sequence of events that lead to cell death in cancer cells depleted of Plk1. Upon depletion of Plk1 DNA damage becomes evident, as detected by phosphorylation of H2A.X. We specifically examined whether activation of enzymes commonly associated with apoptosis precedes or follows DNA damage. We found that DNA damage is an early event and that it leads to activation of ATM, phosphorylation of Chk2 and activation of caspases. Depletion of Plk1 results in the accumulation of Emi1, an APC/C inhibitor, which prevents the destruction of geminin, an inhibitor of pre-replicative complex formation (Fig. 7). Although DNA synthesis is only moderately delayed in Plk1-depleted cells, pre-replication complex formation is disrupted, as shown by underloading of Mcm proteins (See Fig. 4). Mammalian pre-RC assembly takes place during telophase and early G1 phase, mediated by post-translational modifications of pre-existing proteins (23). Plk1 interacts with pre-RC components, and Mcm2-7 and Orc2 proteins colocalize in the centrosome where Plk1 is located at the end of mitosis (32, 35). Based on these reports and our data, Plk1 may phosphorylate pre-RC components during pre-replicative complex formation at replication origins and it may be required for pre-RC assembly. If so, Plk1 depletion itself could lead to the disassembly of pre-RC during the telophase to G1 transition. A recent report shows that Plk1 interacts with and phosphorylates the DNA pre-RC regulatory protein histone acetyltransferase binding to Orc1 (Hbo1) (39). Hbo1 phosphorylation may be required for pre-RC formation, and thus Plk1 may regulate replication licensing by this pathway.

14

A recent report indicates that in *Xenopus* egg extracts Plx1 is required for DNA replication in the presence of stalled replication forks induced by treatment with aphidicolin or etoposide (34). However, that study is fundamentally different from the work presented here, as Plx1 was immunodepleted, which has the potential to remove other proteins that interact with it. Addition of recombinant protein produced in insect cells does not entirely resolve this issue as it, too, may contain Plx1- associated proteins derived from the insect cells. It could be argued that the double thymidine block employed in our experiments results in a stress condition equivalent to that caused by the inhibitors used in the *Xenopus* egg extracts. However, we also observe evidence of DNA damage, as shown by H2A.X phosphorylation and ATM activation, in cells synchronized by serum starvation as they enter S phase at 12 hours after serum stimulation (see Fig. 6). Presumably such synchronized cells represent a normal unperturbed population.

Recent reports show that ATM is activated in response to replication stress (24, 31, 40). ATM is activated during DNA replication stress induced by aphidicolin resulting in fragile site generation, and DNA fragmentation. These results provide evidence for double-stranded DNA breaks and recruitment of phosphorylated ATM to nuclear foci (24). Other reports indicate that replication stress inducers, hydroxyurea and aphidicolin, also activate the ATM-dependent signaling pathway mediated by NF-kB activation. ATM is the essential DNA damage signal transducer for NF-kB activation in response to replication stress (40). Plk1 depletion led to early activation of Chk2 and ATM in G1/S whereas Chk1 activation was undetectable or delayed. These data indicate that Plk1 depletion induced double stranded DNA breaks rather than single-stranded DNA breaks. Plk1 depletion appears to cause pre-replication complex disruption and activate

ATM signaling pathway.

p53, a key regulator of cellular stress, is activated by DNA damage-sensing kinases and checkpoint kinases. We evaluated DNA damage and apoptosis after Plk1 depletion in cancer cells expressing different levels of p53. DNA damage preceded apoptosis and was p53-independent, but the degree of DNA damage and the time of caspase-3 activation were delayed in p53-wt cells as compared to p53-null cancer cells. H1299 p53-null cells displayed more severe accelerated DNA damage and apoptosis than U2OS and HeLa cells. In p53-null cells, DNA damage leading to apoptosis may be mediated by p73; p53 requires p63 and p73 for triggering apoptosis in response to DNA damage (5). However, p73 is pro-apoptotic in the absence of p53 as a result of NOXA transcription and BAX translocation (16, 20). p73 knockdown prevents the expression of NOXA as well as PARP cleavage in p53 deficient HCT 116 cells treated with Nutlin, an apoptotic inducer (16). It has been reported that Chk1/Chk2-driven E2F1 activation and p73 up-regulation in turn lead to expression of pro-apoptotic proteins such as Puma and Bax in p53-independent apoptotic progression (11, 20, 30, 36). Another report indicates that Plk1 phosphorylates p73 protein directly, inhibits its proapoptotic activity and reduces its stability (13). Thus, Plk1 depletion may increase the level of p73 directly or through E2F1. In support of this interpretation, our experiments reveal that the level of p73 increased in Plk1-depleted H1299 cells and the depletion of p73 reduced the expression of Bax.

We have demonstrated that Plk1 depletion induces DNA instability, which may be mediated by the accumulation of Emi1, an inhibitor of APC/C, and geminin, an inhibitor of Pre-RC formation. There is evidence supporting the correlation between Plk1, Emi1, APC/C, and geminin. First, depletion of Cdh1, an APC activator during late

16

mitosis and early G1, induces premature and prolonged S phase, cytokinesis defects, and multipolar mitosis, similar to the Plk1-depletion phenotype (4). These authors suggest that depletion of Cdh1 leads to the stabilization of target proteins of APC/C and thus may initiate aberrant DNA replication and genomic instability. Second, overexpression of non-degradable Emi1, an inhibitor of APC, also results in similar cellular morphology that correlates with the level of Emi1 and the extent of cell death (19). Third, the expression of non-degradable geminin mutated in the destruction box reduces the quantity of Mcm2 bound to chromatin, blocks cell cycle with an early S phase arrest, leads to the activation of checkpoint machinery, and eventually triggers apoptosis in U2OS cells (28). They also show that in primary fibroblasts IMR90, the expression of non-degradable geminin did not induce apoptosis. These phenotypes are very similar to those observed in Plk1-depleted cancer cells compared to normal cells. Thus, the absence of APC/C activation as the result of Emi1 accumulation may contribute to DNA instability and cell death in Plk1-depleted cells.

In summary, Plk1 depletion leads to the accumulation of Emi1 and geminin protein, which appears to contribute to disrupted DNA pre-RC formation, reduced DNA synthesis and subsequent DNA damage before cells undergo severe mitotic catastrophe or apoptosis. Our data suggest that Plk1 is required for accurate cell cycle progression not only in mitosis but also during DNA synthesis.

MATERIALS AND METHODS

Cell culture, Synchronization, and Treatments

HeLa, U2OS, Saos2, T98G and 293T cells were grown in Dulbeco's modified Eagle's medium (Invitrogen; Carlsbad, CA, USA) and H1299 cells were grown in RPMI 1640 medium (ATCC; Manassas, VA, USA) supplemented with 10% fetal bovine serum in the presence of antibiotics in a humidified 5% CO_2 incubator at 37°C. HeLa, U2OS, Saos2, H1299, T98G cells were synchronized with 2.5 mM thymidine (Sigma; St. Louis, MO, USA) for 16 h, released with fresh medium and also infected with lentivirus-expressing RNAi targeting Plk1 at nucleotide 1424 (P), control lentivirus carrying the hairpin-pLKO-puro.1 vector (C), or off-site lentivirus carrying mutant sequence of Plk1 (M). After 8 h, cells were again treated with 2.5 mM thymidine for 16 h, released with fresh medium from the double thymidine block and then samples were prepared at various times. To block cells in G1/early S, cells were treated with 4 mM hydroxyurea (Sigma; St. Louis, MO, USA) for 6 h after release from double thymidine block.

Lentivirus-based RNAi Plasmid Preparation, Virus Production, and Infection.

The lentivirus-based RNAi transfer plasmids targeting human Plk1 at 1424-1444 (AGATCACCCTCCTTAAATATT) (pLKO-Puro.1-Plk1), Plk1 mutant at 1424-1444 (AGAGCACCCTACTTAGATATT) (pLKO-Puro.1-Plk1-mt) for off-site targeting, or control plasmid (pLKO-Puro.1) were prepared and control lentivirus (C), Plk1 targeting lentivirus (P), and off-site lentivirus (M) were generated as described previously (17). Infections were carried out in the presence of 10 μg/ml polybrene and 10 mM HEPES. Selection with puromycin was not carried out because the infection efficiency was high

and puromycin may have unknown secondary effects to DNA damage. Transfections were performed with pEGFP, pEGFP-mouse-Plk1 wild type (WT) or kinase defective mutant (K82M) (12) and Polyfect (Qiagen; Valencia, CA, USA) into the Plk1-depleted or control cells according to the manufacturer's protocols when cells were released from the first thymidine block.

siRNA transfection

For depletion of human p73, H1299 cells were transfected with non-targeting siRNA control (Cat. No. D-001810-01-05; Dharmacon) and human p73 siRNA (target sequence :GAGACGAGGACACGUACUA) from Dharmacon (Lafayette, CO, USA) using Oligofectamin (Invitorgen; Carlsbad, CA, USA) according to the manufacturer's protocols. At 32 h after transfection, cells were synchronized with 2.5 mM thymidine for 16 h, released with fresh medium and infected with lentivirus-expressing RNAi targeting Plk1 (P), or control lentivirus carrying the hairpin-pLKO-puro.1 vector (C). After 8 h, cells were again treated with 2.5 mM thymidine for 16 h, released with fresh medium from the double thymidine block and assayed.

Immunofluorescence

For immunofluorescence, cells grown on coverslips were fixed with 4% paraformaldehyde and permeabilized with methanol. Cells were washed three times with 0.1% Triton X-100 in PBS, incubated overnight at 4°C in 0.1% Triton X-100-PBS containing 3% BSA for blocking, and then incubated with cleaved caspase-3 (D175) polyclonal and p-histone H2A.X (Ser139) monoclonal antibodies from Cell Signaling (Danvers, MA, USA). Cells were washed three times with 0.1% TritonX-100-PBS and

then incubated with CyTM3-conjugated anti-rabbit secondary antibodies (Jackson Immuno Research Laboratories; West Grove, PA, USA) or FITC-conjugated anti-mouse secondary antibodies (Invitrogen; Carlsbad, CA, USA) and 4′, 6- diamidine-2-phenylindole (DAPI) (Sigma; St. Louis, MO, USA) for staining nuclear DNA. Image were collected and analyzed by the Z series of Applied Precision Deconvolution Microscope and Deltavision software.

Fluorescence-activated cell sorting (FACS) analysis

For the determination of the population of subgenomic DNA as an apoptotic index, cells were collected by trypsinization and fixed in 75% ethanol, stained with 500 μl of 50 μg /ml propidium iodide solution, and subjected to FACS analysis. Cells were sorted and analyzed by the Becton Dickinson (Franklin Lakes, NJ, USA) FACScan machine and CellQuest sofeware.

Comet assay

CometAssay^{TM} kit was from Trevigen (Gaithersburg, MD, USA) and the experiments were performed according to the manufacturer's protocols.

Fluorometric caspase-3 activity assay

Fifty μg of whole cell lysates was incubated with 200 nM Ac-DEVD-AMC (BD Biosciences; Franklin Lakes, NJ, USA) in reaction buffer [20 mM Hepes (pH 7.4), 2 mM DTT, 10% glycerol] at 37 °C for 1 h. The reaction was monitored by fluorescence emission at 465 nm (excitation at 360 nm) and measured with a Spectramax Gemini XS Fluorescent Plate Reader.

5-Bromo-2′-deoxy-uridine (BrdU) labeling assay

5-Bromo-2′-deoxy-uridine (BrdU)-labeling and -detection kit was from Roche Applied Science (Indianapolis, IN, USA). The assay was carried out according to the manufacturer's protocols.

Chromatin-Binding Assay

Chromatin was fractionated with Triton X-100. The soluble fraction of cells was prepared by lysis in 200 μl CSK buffer [10 mM PIPES (pH 6.8), 100 mM NaCl, 300 mM sucrose, 3 mM $MgCl_2$, 1 mM EGTA, 1 mM DTT, 1 mM PMSF, 50 mM NaF, 0.1 mM sodium vanadate, 0.5% Triton X-100 and protease inhibitor cocktail (Roche; Indianapolis, IN, USA)] for 5 min on ice. Cell lysates were centrifuged at 7,500 rpm for 5 min at 4°C and the supernatants were collected. The chromatin pellet was washed again with CSK buffer and centrifuged at 7,500 rpm for 5 min at 4°C. For nuclease digestions, chromatin pellets were resuspended in lysis buffer containing 30 units of micrococcal nuclease (Roche; Indianapolis, IN, USA) and 1 mM $CaCl_2$ and then incubated at 37°C for 10 min followed by chilling on ice and centrifugation. After adjusting the protein concentration, proteins were resolved by SDS-PAGE and analyzed by western blot with anti-Mcm7 (Santa Cruz; Santa Cruz, CA, USA), anti-Mcm3 (BioLgend, San Diego, CA, USA), anti-nucleophosmin (Zymed; Carlsbad, CA, USA), anti-Plk1 (Upstate; Billerica, MA, USA), anti-Erk2 (Santa Cruz; Santa Cruz, CA, USA) anti-geminin, and anti-Cdt1 (Bethyl Lab, Montgomery, TX, USA) antibodies. For immunoprecipitation assays, geminin was immunoprecipitated from soluble fraction with anti-geminin antibody (Bethyl Lab, Montgomery, TX, USA) for 4 h at 4°C with

end-over-end mixing, followed by incubation with protein A agarose (Upstate; Billerica, MA, USA) for 2 h at 4°C. Immunoprecipitates were subjected to immunoblot with anti-geminin and anti-Cdt1 antibodies.

Kinase assay

ATM was immunoprecipitated from cell lysates with an anti-ATM polyclonal antibody (Santa Cruz; CA, USA) for 4 h at 4°C with end-over-end mixing, followed by incubation with protein A agarose (Upstate; Billerica, MA, USA) for 2 h at 4°C. Immunoprecipitates were separated from supernatants by centrifugation and washed with lysis buffer. The reaction for ATM activity was performed as described (41). The samples were suspended in SDS loading buffer, resolved by SDS-PAGE and detected by autoradiography.

Immunoblot analysis

Cells were collected and extracted in lysis buffer [0.5% Triton X-100, 20 mM Tris, pH 7.5, 2 mM $MgCl_2$, 1 mM dithiothreitol (DTT), 1 mM EGTA, 50 mM β-glycerophosphate, 25 mM NaF, 1 mM Na vanadate, 100 μg/ml PMSF, and protease inhibitor cocktail (Roche; Indianapolis, IN, USA)]. After adjusting the protein concentration, proteins were resolved by SDS-PAGE and analyzed by western blot analysis with the appropriate antibodies. Anti-Erk2, anti-Chk2, and anti-Bax polyclonal antibodies and anti-cyclin B1 and anti-E2F1 monoclonal antibodies were from Santa Cruz (Santa Cruz, CA, USA). Anti-Plk1 monoclonal from Upstate (Billerica, MA, USA), anti-p-Chk2 (T68), and anti-p-Chk1 (S345) polyclonal from Cell Signaling (Danvers, MA, USA), anti-p53 monoclonal from Oncogene (San Diego, CA, USA),

22

anti-p-ATM (S1981) monoclonal from Calbiochem (Gibbstown, NJ, USA), anti-geminin polyclonal from Bethyl Lab (Montgomery, TX, USA), anti-p73 and anti-Emi1 polyclonal antibodies from Zymed (Carlsbad, CA, USA) were used. Immune complexes were revealed using Amersham ECL^{TM} western blotting detection reagents (GE Healthcare; Piscataway, NJ, USA).

ACKNOWLEDGMENTS

REFERENCES

1. Cogswell, J. P., Brown, C. E., Bisi, J. E. and S. D. Neill. 2000. Dominant-negative polo-like kinase 1 induces mitotic catastrophe independent of cdc25c function. *Cell Growth & Differentiation.* 11: 615-623.

2. Diffley, J. F. 2004. Regulation of early events in chromosome replication. *Curr. Biol.* 14: R778-786.

3. Eckerdt, F., Yuan, J. and K. Strebhardt. 2005. Polo-like kinase and oncogenesis. *Oncogene* 24:267-276.

4. Engelbert, D., Schnerch, D., Baumgarten, A. and R. Wäsch. 2008. The ubiquitin ligase APC (Cdh1) is required to maintain genome integrity in primary human cells. *Oncogene* 27:907-917.

5. Flores, E. R., Tsai, K. Y., Crowley, D., Sengupta, S., Yang, A., Mckeon, F. and T. Jacks. 2002. p63 and p73 are required for p53-dependent apoptosis in response to DNA damage. *Nature* 416:560-564.

6. Fry, A. M. and H. Yamano. 2006. APC/C-mediated degradation in early mitosis. *Cell Cycle* 14:1487-1491.

7. Glover, D. M. 2005. Polo kinase and progression through M phase in *Drosophila*: a

perspective from the spindle poles. *Oncogene* 24:230-237

8. Golsteyn, R. M., Mundt, K. E., Fry, A. M. and E. A. Nigg. 1995. Cell cycle regulation of activity and subcellular localization of Plk1, a human protein kinase implicated in mitotic spindle function. *J. Cell Biol.* 129:1617-1628.

9. Hamanaka, R., Maloid, S., Smith, M. R., O'Connell, C. D., Longo, D. L. and D. K. Ferris. 1994. Cloning and characterization of human and murine homologues of the Drosophila polo serine-threonine kinase. *Cell Growth Differ.* 5:249-257.

10. Hansen, D. V., Loktev, A. V. Ban, K. H. and P. K. Jackson. 2004. Plk1 regulates activation of the anaphase promoting complex by phosphorylating and triggering SCFbetaTrCP-dependent destruction of the APC Inhibitor Emi1. *Mol. Biol. Cell* 15:5623-5624.

11. Irwin, M., Marin, M. C., Phillips, A. C., Seelan, R. S., Smith, D. I., Liu, W., Flores, E.R., Tsai, K. Y., Jacks, T., Vousden, K. H. and W. G.. Jr. Kaelin. 2002. Role for the p53 homologue p73 in E2F-1-induced apoptosis. *Nature* 407:645-648.

12. Jang, Y.-J., Ma, S. Terada, Y. and R. L. Erikson. 2002. Phosphorylation of threonine 210 and the role of serine 137 in the regulation of mammalian polo-like kinase. *J. Biol. Chem.* 277:44115-44120.

13. Koida, N., Ozaki, T., Yamamoto, H., Ono, S., Koda, T., Ando, K., Okoshi, R.,

Kamijo, T, Omura, K. and A. Nakagawara. 2008. Inhibitory role of Plk1 in the regulation of p73-dependent apoptosis through physical interaction and phosphorylation. *J. Biol. Chem.* 283:85555-8563.

14. Kumagai, A. and W. G. Dunphy. 1996. Purification and molecular cloning of Plx1, a Cdc25-regulatory kinase from Xenopus egg extracts. *Science* 273:1377-1380.

15. Lane, H. A. and E. A. Nigg. 1996. Antibody microinjection reveals an essential role for human polo-like kinase 1 (Plk1) in the functional maturation of mitotic centrosome. *J. Cell Biol.* 135:1701-1713.

16. Lau, L. M., Nugent, J. K., Zhao, X., and M. S. Irwin. 2008. HDM2 antagonist Nutlin-3 disrupts p73-HDM2 binding and enhances p73 function. *Oncogene* 27: 997-1003.

17. Liu, X., Lei, M. and R. L. Erikson. 2006. Normal cells, but not cancer cells, survive severe Plk1 depletion. *Mol. Cell. Biol.* 26:2093-2108.

18. Liu, X. and R. L. Erikson. 2003. Polo-like kinase (Plk)1 depletion induces apoptosis in cancer cells. *Proc. Natl. Acad. Sci. USA* 100:5789-5794.

19. Margottin-Goguet, F., Hsu, J. Y., Loktev, A., Hsieh, H. M., Reimann, J. D. and P. K. Jacskon. 2003. Prophase destruction of Emi1 by the SCF (betaTrCP/Slimb) ubiquitin

ligase activates the anaphase promoting complex to allow progression beyond prometaphase. *Dev. Cell* 4:813-826.

20. Melino, G., Bernassola, F., Ranalli, M., Yee, K., Zong, W. X., Corazzari, M., Knight, R. A., Green, D. R., Thompson, C. and K. H. Vousden. 2004. p73 induces apoptosis via PUMA transactivation and Bax mitochondrial translocation. *J. Biol. Chem*. 279:8076-8083.

21. Moller, P. 2006. The alkaline comet assay: towards validation in biomonitoring of DNA damaging exposures. *Basic Clin Pharmacol Toxicol.* 98:336-345.

22. Moshe, Y., Boulaire, J., Pagano, M. and A. Hershko. 2004. Role of Polo-like kinase in the degradation of early mitotic inhibitor 1, a regulator of the anaphase promoting complex/cyclosome. *Proc. Natl. Acad. Sci. USA.* 101:7937-7942.

23. Okuno, Y., McNairn, A. J., den Elzen, N., Pines, J. and D. M. Gilbert. 2001. Stability, chromatin association and functional activity of mammalian pre-replicative complex proteins during the cell cycle. *EMBO J.* 20:4263-4277.

24. Ozeri-Galai, E., Schwartz, M., Rahar, A. and B. Kerem. 2008. Interplay between ATM and ATR in the regulation of common fragile site stability. *Oncogene* 27: 2109-2117.

25. Prasanth, S. G., Prasanth, K. V., Siddiqui, K., Spector, D. L. and B. Stillman. 2004.

Human Orc2 localizes to centrosomes, centromeres and heterochromatin during chromosome inheritance. *EMBO J.* 23:2651-2663.

26. Reimann, J. D., Freed, E., Hsu, J. Y., Kramer, E. R., Peters, J. M. and P. K. Jackson. 2001. Emi1 is a mitotic regulator that interacts with Cdc20 and inhibits the anaphase promoting complex. *Cell* 105:645-655.

27. Roos, W. P. and B. Kaina. 2006. DNA damage-induced cell death by apoptosis. *Trends in Molecular Medicine* 12:1471-1476.

28. Shreeram, S., Sparks, A., Lane, D. P., and J. J. Blow. 2002. Cell type-specific responses of human cells to inhibition of replication licensing. *Oncogene* 21: 6624-6632.

29. Smits, V. A. and R. H. Medema. 2001. Checking out the G2/M transition. *Biochim. Biophys. Acta.* 1519:1-12.

30. Stevens, C., Smith, L. and N. B. La Thangue. 2003. Chk2 activates E2F-1 in response to DNA damage. *Nat. Cell Biol.* 5:401-409.

31. Stiff, T., Walker, S. A., Cerosaletti, K., Goodarzi, A. A., Petermann, E., Concannon, O., O'Driscoll, M., and P. A. Jeggo. 2006. ATR-dependent phosphorylation and activation of ATR in response to UV treatment or replication fork stalling. *EMBO J.* 25: 5775-5782.

32. Stuermer, A., Hoehn, K., Faul, T., Auth, T., Brand, N., Kneissl, M., Putter, V. and F. Grummt. 2007. Mouse pre-replicative complex proteins colocalise and interact with the centrosome. *Eur. J. Cell Biol.* 86:37-50

33. Sumara, I., Gimenez-Abian, J. F., Gerlich, D., Hirota, T., Kraft, C., de la Torre, C., Ellenberg, J. and J. M. Peters. 2004. Roles of polo-like kinase 1 in the assembly of functional mitotic spindles. *Curr. Biol.* 14:1712-1722.

34. Trenz, K., Errico, A. and V. Costanzo. 2008. Plx1 is required for chromosomal DNA replication under stressful conditions. *EMBO J.* 27:876-885.

35. Tsvetkov, L. and D. F. Stern. 2005. Interaction of chromatin-associated Plk1 and Mcm7. *J. Biol. Chem.* 280:11943-11947.

36. Urist, M., Tanaka, T., Poyurovsky, M. V. and C. Prives. 2004. p73 induction after DNA damage is regulated by checkpoint kinases Chk1 and Chk2. *Genes Dev.* 28:3041-3054.

37. van Vugt, M. A. T. M. and R. H. Medema. 2005. Getting in and out of mitosis with Polo-like kinase-1. *Oncogene* 24:2844-2859.

38. van Vugt, M. A., van de Weerdt, B. C., Janssen, H., Calafat, J., Klompmaker, R., Wolthuis, R. M. and R. H., Medema. 2004. Polo-like kinase 1 is required for bipolar spindle formation but is dispensable for anaphase promoting complex/cdc20 activation

and initiation of cytokinesis. *J. Biol. Chem.* 279:36841-36853.

39. Wu, Z. and X. Liu. 2008. Role for Plk1 phosphorylation of Hbo1 in regulation of replication licensing. *Proc. Natl. Acad. Sci. U S A.* 105:1919-1924.

40. Wu, Z.-H., and S. Miyamoto. 2008. Induction of a pro-apoptotic ARM-NF-kB pathway and its repression by ATR in response to replication stress. *EMBO J.* 27: 1963-1973.

41. Yim, H., Hwang, I. S., Choi, J. S., Chun, K. H., Jin, Y. H., Ham, Y. M., Lee, K. Y. and S. K. Lee. 2006. Cleavage of Cdc6 by caspase-3 promotes ATM/ATR kinase-mediated apoptosis of HeLa cells. *J. Cell Biol.* 174:77-88.

Figure Legends

Figure 1. The formation of γ-H2A.X foci precedes the activation of caspase-3 in Plk1-depleted HeLa cells. HeLa cells were synchronized with double thymidine block and infected with either lentivirus expressing RNAi targeting Plk1 (P) or control (C) as described in Materials and methods. Note: Zero time of release is 24 hrs after infection. **(A)** Whole cell lysates were subjected to immunoblot analysis with anti-Plk1 and anti-Erk2 antibodies. **(B)** FACS analysis of cell cycle progression. **(C)** HeLa cells grown on coverslips were fixed with 4% paraformaldehyde and examined for phosphorylated H2A.X (Green) or cleaved caspase-3 (Red). Nuclear DNA was stained with DAPI. The scale bar indicates 10 μm. **(D-E)** The γ-H2A.X- and cleaved caspase-3-positive cells were counted and quantified.

Figure 2. The involvement of p53 and p73 in DNA damage induced by Plk1 depletion. Cells were synchronized with double thymidine block and infected with lentivirus-expressing RNAi targeting Plk1 or control. **(A-B)** The γ-H2A.X- or cleaved caspase-3-positive cells were counted and quantified. **(C)** FACS analysis of cell cycle progression in Plk1-depleted H1299 cells. **(D)** Extracts of H1299 cells were subjected to immunoblot analysis with anti-p-Chk2 (T68), anti-E2F1, anti-p73, anti-p-Chk1 (S345), anti-Plk1 and anti-Erk2 antibodies. **(E-G)** H1299 cells were transfected with human p73 siRNA and infected with human Plk1 targeting lentivirus during the double thymidine block as described in Materials and methods. **(E-F)** At 12 h and 24 h after release from the double thymdine block, cells were prepared and FACS analysis was performed. The subgenomic DNA was quantified. **(G)** At 12 h after release from the double thymidine

32

block, extracts were subjected to immunoblot analysis with anti-p73, anti-Plk1, anti-Bax, and anti-Erk2 antibodies.

Figure 3. DNA damage occurs in G1/early S phase in HeLa cells. HeLa cells were synchronized with double thymidine block and infected with lentivirus-based RNAi targeting Plk1 (P) or with control (C) virus. **(A-B)** Cells were released with fresh medium in the presence or absence of hydroxyurea. Cells with DNA damage are visualized by the comet assay, and quantified. The scale bar indicates 50 μm. **(C)** FACS analysis of the cells shown in (A) and (B). **(D)** The γ-H2A.X-positive cells were counted and quantified at the indicated times.

Figure 4. Plk1 depletion inhibits DNA synthesis and disrupts the binding of Mcm proteins to chromatin in early S phase. HeLa cells were synchronized and infected as described in Materials and methods. **(A-B)** At 1 h or 1 h 30 min after release, 5'-bromo-2'-deoxy-uridine (BrdU) was added to the cells, and after 60 min or 30 min, the cells were fixed and labeled with anti-BrdU antibody (Green). Nuclear DNA was stained with DAPI. The scale bar indicates 50 μm. The 5'-bromo-2'-deoxy-uridine (BrdU)-positive cells were counted and quantified. **(C)** At 2 h after release, cells were fractionated into soluble and chromatin fractions as described in Materials and methods, and subjected to immunoblot with anti-Mcm7, anti-Mcm3, anti-nucleophosmin, anti-Plk1, and anti-Erk2 antibodies. **(D)** HeLa cells were infected with Plk1-targeting lentivirus or control virus. After 8 h, cells were treated with thymidine for 16 h and then transfected with pEGFP, pEGFP-Plk1-wild type (WT), or pEGFP-Plk1-K82M (KM). Murine Plk1 is resistant to human Plk1 RNAi. After 8 h, the cells were again treated

with thymidine for 16 h and then released with fresh medium. At 2 h after release, cells were fractionated into soluble and chromatin fractions and subjected to immunoblot with anti-Mcm7, anti-nucleophosmin, anti-Plk1, and anti-Erk2 antibodies. **(E)** At 2 h after release, extracts were subjected to ATM or ATR assay using anti-ATM antibody or anti-ATR antibody, respectively. The kinase activity was measured with PHAS-1 as a substrate. PHAS-1 was visualized by staining with coomassie brilliant blue.

Figure 5. Plk1 depletion results in a high level of Emi 1 and geminin. (A) HeLa cells were synchronized and infected as described in Materials and methods. Whole cell lysates were subjected to immunoblot analysis with anti-Emi1, anti-geminin, anti-cyclin B1, anti-Plk1, anti-Erk2, anti-p-ATM (S1981), anti-p-Chk2 (T68), and anti-Chk2 antibodies. **(B)** HeLa cells grown on coverslips were infected, synchronized and transfected as described in Figure 4D. At 2 h after release, cells were fixed with 4% paraformaldehyde and examined GFP (Green) or Emi1 (Red). Nuclear DNA was stained with DAPI. The scale bar indicates in 10 μm. **(C)** HeLa cells were synchronized and infected as described in Materials and methods. At 2 h after release, cells were fractionated into soluble and chromatin fractions, and subjected to immunoblot with anti-Cdt1, anti-geminin, anti-Plk1, and anti-Erk2 antibodies **(D)** The soluble extracts were subjected to immunoprecipitation assay using anti-geminin antibody and subjected to immunoblot with anti-Cdt1 and anti-geminin antibodies.

Figure 6. DNA damage occurred in G1/ S transition and DNA synthesis was reduced in Plk1-depleted T98G cells. T98G cells were synchronized with serum starvation for 2 days and infected with lentivirus-based RNAi targeting Plk1 (P) or with

control virus (C) in serum free medium for 1 day. Cells were released with fresh medium containing 10% fetal bovine serum and then harvested at various times. **(A)** Extracts were subjected to ATM assay using anti-ATM antibody with PHAS-1 as substrate. PHAS-1 was visualized by staining with coomassie brilliant blue. Also immunoblot analysis was performed with anti-Plk1 and anti-Erk2 antibodies. **(B)** DNA damage was measured by immunohistochemistry using γ-H2A.X monoclonal antibody. The γ-H2A.X-positive cells were counted and quantified. **(C)** FACS analysis was performed. **(D)** At 16 h after release, 5'-bromo-2'-deoxy-uridine (BrdU) was added to the cells. After 30 min, cells were fixed and labeled by anti-BrdU antibody (Green). Nuclear DNA was stained by DAPI. The scale bar indicates 20 μm. **(E)** The 5'-bromo-2'-deoxy-uridine (BrdU)-positive T98G cells were counted and quantified. **(F)** T98G cells were synchronized with serum starvation for 2 days and infected as described above. Whole cell lysates were subjected to immunoblot analysis using anti-p-ATM (S1981), anti-Emi1, anti-geminin, anti-Plk1, and anti-Erk2 antibodies. **(G)** T98G cells were synchronized with double thymidine block and infected with lentivirus as described above. Lysates were subjected to immunoblot analysis using anti-p-Chk2 (T68), anti-Emi1, anti-Plk1, and anti-Erk2 antibodies.

Figure 7. A model for the mechanism of DNA damage and cell death induced by Plk1 depletion. Under normal conditions, Plk1 phosphorylates Emi1, which results in degradation of Emi1 and activation of APC/C. Activated APC/C degrades the mitotic proteins such as cyclin B1 and geminin at the end of mitosis leading to exit from M phase. Upon Plk1 depletion, Emi1 is not phosphorylated by Plk1, which results in the accumulation of Emi1. The high level of Emi1 inhibits the APC/C activity, which leads

to a high level of geminin, an inhibitor of pre-replicative complex. Consequently, geminin disrupts the pre-RC and DNA-damage-sensing kinases are activated.

Supplementary Figure Legends

Figure S1. Plk1 depletion induces apoptosis in HeLa cells. HeLa cells were infected with either lentivirus expressing RNAi targeting Plk1 (P), control (C), Plk1 mutant for off-site targeting (M) and selected with puromycin for 2 days. Cells were prepared at 3, 4, or 5 days after infection. **(A)** FACS analysis of cell cycle progression. **(B)** Cell extracts were assayed for caspase-3 activity. Cell lysates treated with 50 μM etoposide for 20 h were used as a positive control for caspase-3 activity. RFU, relative fluorescence unit. **(C)** At 3 days after infection, HeLa cells grown on coverslips were fixed with 4% paraformaldehyde and examined for phosphorylated H2A.X (Green) or cleaved caspase-3 (Red). Nuclear DNA was stained with DAPI. The scale bar indicates 20 μm. **(D)** The γ-H2A.X- and cleaved caspase-3-positive cells were counted and quantified.

Figure S2. The activation of caspase-3 enzyme in Plk1-depleted and puromycine non-selected HeLa cells. Cells were synchronized with double thymidine block and infected with lentivirus expressing RNAi targeting Plk1 or control as described in Materials and methods. Note: Zero time of release is 24 hrs after infection. **(A)** The scheme of experiment. **(B)** Cell extracts were assayed for caspase-3 activity at the indicated times. RFU, relative fluorescence unit.

Figure S3. The γ-H2A.X foci formed in Plk1-depleted HeLa cells. HeLa cells were synchronized and infected as described in Materials and methods. At 10h after release from double thymidine block, HeLa cells grown on coverslips were fixed with 4%

paraformaldehyde and examined phosphorylated H2A.X (Green) or Plk1 (Red). Nuclear DNA was stained with DAPI. The scale bar indicates 10 μm.

Figure S4. Plk1 depletion results in a high level of Emi 1 and geminin. HeLa cells were infected with Plk1 targeting lentivirus or control virus. After 8 h, cells were treated with thymidine for 16 h and then transfected with pEGFP, pEGFP-Plk1-wild type (WT), or pEGFP-Plk1-K82M (KM). After 8 h, the cells were again treated with thymidine for 16h and then released with fresh medium. At 2 h after release, cells were prepared and extracts were subjected to immunoblot analysis with anti-Emi1, anti-geminin, anti-Plk1, and anti-Erk2 antibodies.

Figure 1.

A

B

C

D

E

Figure 2.

Figure 3.

A

B

C

D

Figure 4.

A

B

C

E

D

Figure 5.

A

	0h		2h	
	Con	Plk1-	Con	Plk1-

Emi1

geminin

cyclin B1

Plk1

Erk2

p-ATM (S1981)

p-Chk2 (T68)

Chk2

After release from double thymidine block

C

	Soluble		Chromatin	
	Con	Plk1-	Con	Plk1-

Cdt1

geminin

Plk1

Erk2

D

	Soluble			
	IP: IgG		IP: geminin	
	C	P	C	P

Cdt1 →

IgG →

geminin

B

Control				Plk1-			
DAPI	GFP	Emi1	Merge	DAPI	GFP	Emi1	Merge

GFP

GFP-Plk1-WT

GFP-Plk1-KM

10μm

Figure 6.

A

ATM kinase activity (PHAS-1)

Coomassie Blue Staining (PHAS-1)

Coomassie Blue Staining (IgG heavy chain)

IB : Plk1

IB :Erk2

B

C

D

DAPI

BrdU

Merge

E

F

p-ATM (S1981)

Emi1

geminin

Plk1

Erk2

At 16h after serum stimulation from serum starvation

G

p-Chk2 (T68)

Emi1

Plk1

Erk2

After serum release from double thymidine block

Figure 7

Normal condition

Degradation

Emi1 (P)

Plk1

Emi1

APC Inactive

APC Active

geminin

Degradation

Pre-RC

Cell cycling

Depletion of Plk1

Emi1 (P)

Plk1

Emi1

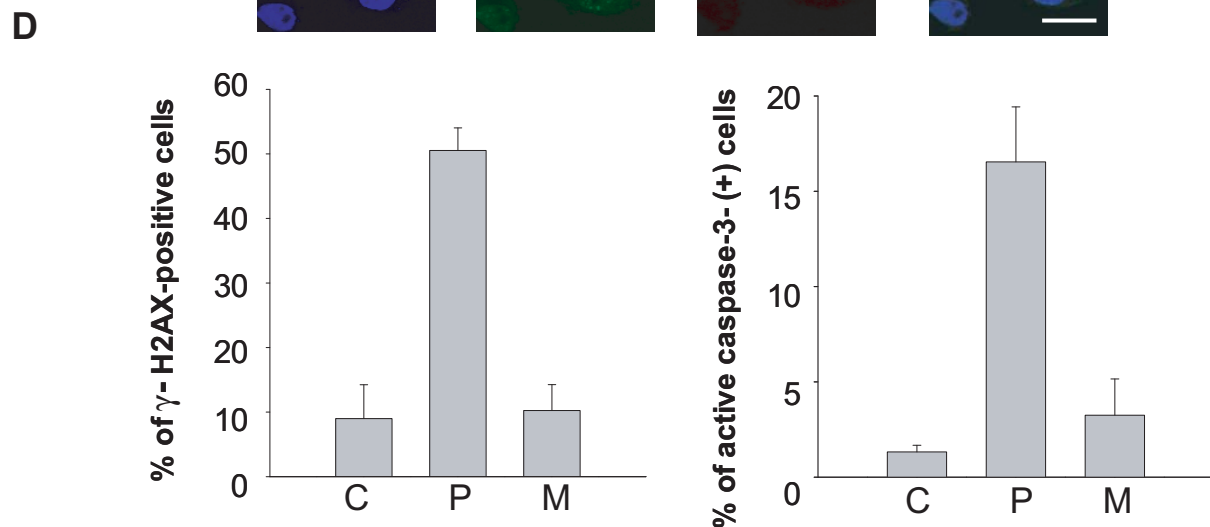Emi1

APC Inactive

geminin

geminin

geminin

Cdt1

Pre-RC

Disrupted chromatin structure

DNA damage

Apoptosis

Supplementary Figure 1.

A

	Con	Plk1-
3D		
4D		
5D		

G1 G2/M   G1 G2/M

B

C

	DAPI	γ-H2AX	caspase-3	merge
Con (vector)				
Plk1-				
Plk1-Mt- (off-target)				

D

Supplementary Figure 2.

A

Split HeLa cells
↓ 24 h
1st thymidine block
↓ 16 h
Release and infection with pLKO-puro1. or -Plk1 virus
↓ 8 h
2nd thymidine block at the same day
↓ 16 h
Release and prepare the sample
in a time course

B

Supplementary Figure 3.

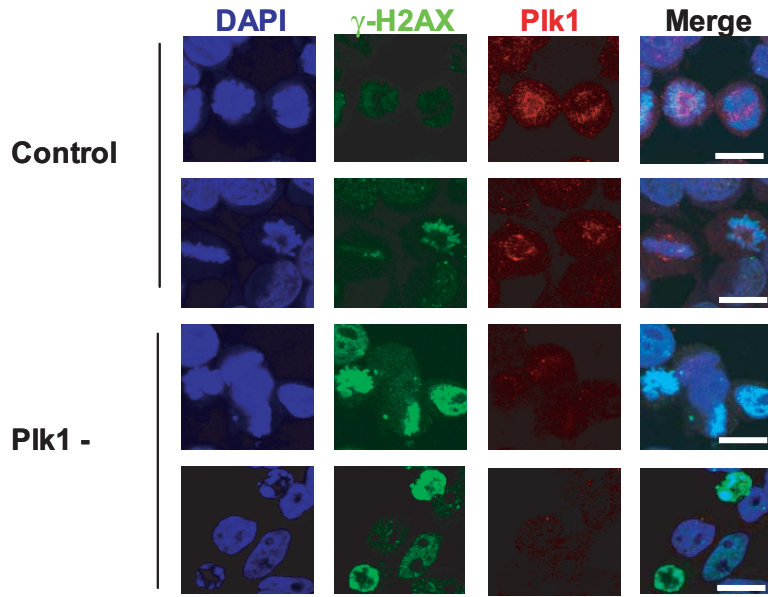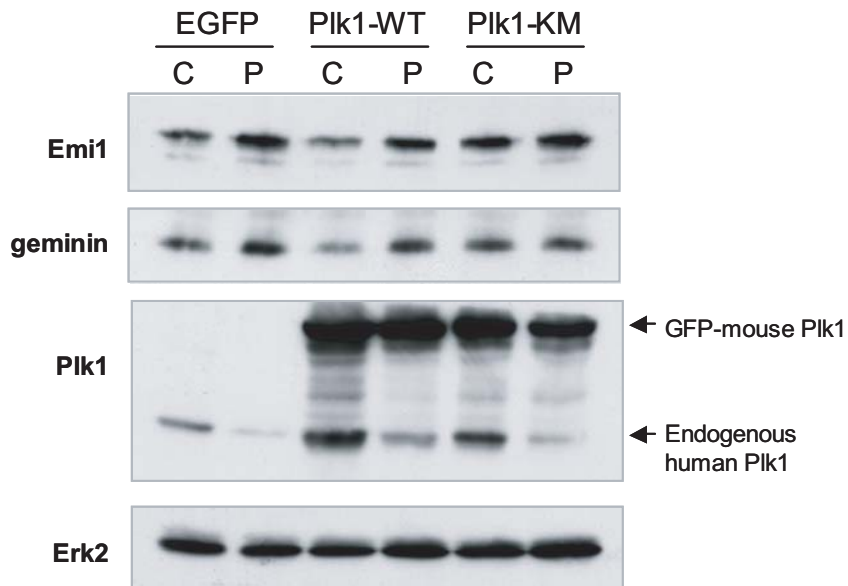|	DAPI	γ-H2AX	Plk1	Merge
Control				
Plk1 -				

At 10 h after release from the double thymidine block

Supplementary Figure 4.

At **2**h after release from thymidine double block